Pergamon

Int. J. Solids Structures Vol. 34, No. 8, pp. 991–1005, 1997

0020–7683/97 $17.00 + .00

PII: S0020–7683(96)00041–8

EDGE FUNCTION ANALYSIS OF GLACIER MECHANICS PROBLEMS

JERRY F. DWYER,† BERNARD AMADEI, C. T. LIN
University of Colorado, Department of Civil Engineering, Boulder, CO 80309, U.S.A

and

W. TAD PFEFFER
University of Colorado, INSTAAR and Department of Geological Sciences

(*Received* 16 *May* 1995; *in revised form* 18 *March* 1996)

Abstract—The edge function method is considered for the analysis of plane strain problems in glacier mechanics. The essence of the approach is the approximation of the solution by a linear combination of analytical solutions (based on the complex variable formulation of anisotropic elasticity) of the field equations. The unknowns in the linear combination are obtained from a system of equations which follows from the approximation of the boundary conditions by a boundary Galerkin energy method. A range of representative glacier geometries are examined and the presence of areas of tension on the surface is evident. The introduction of small crevasses in the form of widely spaced notches does not seem to have a significant effect in the reduction of that tension, away from the notches. A comparison with a finite element approach indicates that an accurate solution is obtained from the edge function method with fewer degrees of freedom and reduced setup effort. The method is well suited to capturing the singularity at the tip of the crevasse but is limited to wide crevasses and the examination of realistic narrow crevasses would be handled more optimally by a combination of the edge function method with its local accuracy and a conventional method with more robust general geometry capabilities.

1. INTRODUCTION

It is generally well-accepted that the calving of icebergs from large glaciers and ice sheets is an important problem currently facing glaciological modelers. Iceberg calving accounts for roughly half of the ablation from Greenland and most of the ablation from Antarctica. Environmentalists are concerned by the uncertain contributions of these huge ice masses to the current worldwide rise in sea level. Additionally, floating iceberg debris presents a potential safety hazard, both to shipping and to off-shore platforms.

Despite the importance of calving in global glacier mass balance, little is understood about the nature of the calving process or the role of calving in glacier dynamics. The majority of dynamical models have not been linked with a calving model in a way that provides realistic physics. As a result, an initiative to address this gap is currently underway at the University of Colorado. Innovative numerical modeling of solid mechanics fracture behavior is taking place with a view to incorporating such models into conventional well-proven finite element models of glacier flow, including quasi-three-dimensional continuity models (Fastook and Chapman, 1987) and vertical plane strain models (Raymond, 1978, 1987). The new approaches to the fracture problem include the Boundary Element method (BEM), the Edge Function method (EFM) and the Discontinuous Deformation Analysis method (DDA).

The first step in the current analysis is to use the new methods to examine some restricted glacier behavior, without any coupling to the glacier flow models. This should add to the existing literature which includes the seminal work of Reeh (1968) who deduced the bending stresses that could cause fracture and calving on a floating beam of ice. Several

† Department of Mechanical Engineering, University of New Hampshire, Durham, NH 03824, U.S.A.

researchers (e.g. Holdsworth, 1969, 1977 and Hughes, 1983, 1992) have provided further insight into the problem defined by Reeh. Fracture in ice has been addressed from the theoretical microscale perspective of the fracture toughness (Hooke *et al.*, 1980), from the experimental perspective (Schulson *et al.*, 1989, Schulson, 1991) and from the macroscale perspective of engineering studies of sea ice (Hocking *et al.*, 1985). The work described in this paper involves an examination of the stresses in an intact glacier, followed by the study of the effect of fracture, in the form of a crevasse, on those stresses. This research was carried out using the EFM. Future papers will report an extension of the modeling using the BEM method, as well as the coupling of these approaches with the FEM flow models.

The edge function technique involves the use of analytical solutions to model the field behavior in various parts of the domain under investigation. The essence of the edge function approach is the approximation of the solution of a boundary value problem by a linear combination of solutions of the field equations. A set of solutions is generated which can model arbitrary effects on each boundary (edge functions) and which exhibit rapid decay away from that boundary. Singular solutions corresponding to vertices, cracks, holes and concentrated loads are also included to provide a rapidly convergent analytical solution. The edge functions and singular solutions are based on the complex variable formulation (Lekhnitskii, 1963). The unknowns in the linear combination are obtained from a system of equations which follows from the approximation of the boundary conditions by a boundary Galerkin energy method.

The edge function method was first developed to solve the torsion problem (Quinlan, 1964) and has been extended to several other areas including three-dimensional elasticity (Grannell *et al.*, 1979), orthotropic plate vibrations (O'Callaghan and Studdert, 1985) and plane problems of anisotropic elasticity (Grannell and Dwyer, 1989). In the latter papers, a range of singular problems is solved. These include problems with mixed boundary conditions, singular loads and elliptical cutouts as well as arbitrarily oriented cracks. Accurate values are obtained for stress intensity factors, using much smaller system matrices than those encountered in other methods. More recent work includes the modeling of gravity forces and this has enabled a study of problems in rock mechanics (Dwyer and Amadei, 1995a, b).

Some notable features of the edge function approach include the high level of accuracy achieved for singular problems and the small number of degrees of freedom required for such accuracy. The method can easily be coupled with conventional finite element schemes, with the edge function technique used to model the singular behavior and far field behavior modeled by finite elements. The current program handles general anisotropic material data but it has also been found (Grannel and Quinlan, 1980) that isotropic materials are efficiently modeled simply by slightly perturbing the elasticities in the material matrix.

The following sections briefly describe the major features of the EFM. The assumptions inherent in the use of the model are then discussed. A range of examples are presented which examine the stress distribution in several glacier geometries. The modified stress pattern, induced by the formation of crevasses is also discussed. Finally, the limitations of the approach are mentioned and the options for continued research are discussed.

2. COMPLEX POTENTIAL FORMULATION OF ANISOTROPIC GENERALIZED PLANE STRAIN

This section summarizes the formulation of the complex variable approach to anisotropic elasticity due to Lekhnitskii (1963). The modern subscript notation and the implied summation convention are adopted. In this paper, tensile normal stresses are taken to be positive.

Consider a cylindrical anisotropic body which is deformed by body forces and surface tractions which act in a plane normal to the generators but do not vary along the generators. The deformation of the body is described in an (x_1, x_2, x_3) Cartesian coordinate system where the x_3-axis is parallel to the generators. The body is assumed to deform under a condition of *generalized plane strain* in the (x_1, x_2) plane. In the (x_1, x_2, x_3) coordinate system, the components of displacement and strain are

$$u_i = u_i(x_1, x_2) \tag{1}$$

and

$$\varepsilon_{ij} = \frac{(u_{i,j} + u_{j,i})}{2} \tag{2}$$

respectively (with $i,j = 1-3$). The constitutive model for the anisotropic medium is described by Hooke's law which can be written in matrix form as follows

$$\boldsymbol{\sigma} = \mathbf{C}\boldsymbol{\varepsilon} \tag{3}$$

or

$$\boldsymbol{\varepsilon} = \mathbf{A}\boldsymbol{\sigma} \tag{4}$$

where

$$\boldsymbol{\varepsilon} = (\varepsilon_{11}, \varepsilon_{22}, \varepsilon_{33}, 2\varepsilon_{23}, 2\varepsilon_{13}, 2\varepsilon_{12})^{\mathrm{T}}$$

are the strain components and

$$\boldsymbol{\sigma} = (\sigma_{11}, \sigma_{22}, \sigma_{33}, \sigma_{23}, \sigma_{13}, \sigma_{12})^{\mathrm{T}}$$

are the stress components. **A** is a (6×6) symmetric compliance matrix with 21 independent components a_{ij} $(i,j = 1,6)$ and **C** is the corresponding matrix of elastic parameters with components c_{ij} $(i,j = 1,6)$ and is such that $\mathbf{C} = \mathbf{A}^{-1}$. The stresses must satisfy the equilibrium equation given by

$$\sigma_{ij,j} + f_i = 0 \tag{5}$$

where $f_i (i = 1-3)$ are the components of the body force vector **f**. In general, a particular integral can be developed to model the body force. The boundary conditions can then be modified to yield a boundary value problem with zero body forces (Dwyer, 1986). In this case, it follows from Lekhnitskii (1963) that the stresses and displacements have the following complex potential representations

$$\sigma_{ij} = \mathrm{Re} \sum_{k=1}^{3} s_{ijk} \Phi'_k(z_k) \tag{6}$$

and

$$u_i = \mathrm{Re} \sum_{k=1}^{3} p_{ik} \Phi_k(z_k) \tag{7}$$

where Re denotes the real part of a complex function and $\Phi'_k(z_k)$ $(k = 1,2,3)$ denotes the derivatives of three analytical stress functions $\Phi_k(z_k)$ of the variable $z_k = x_1 + \mu_k x_2$ where x_1 and x_2 are the coordinates of the point in the anisotropic medium at which the stresses and displacements are calculated. The parameters μ_k $(k = 1,2,3)$ are complex numbers with positive imaginary parts and are the roots of a characteristic equation of the form (Lekhnitskii, 1963)

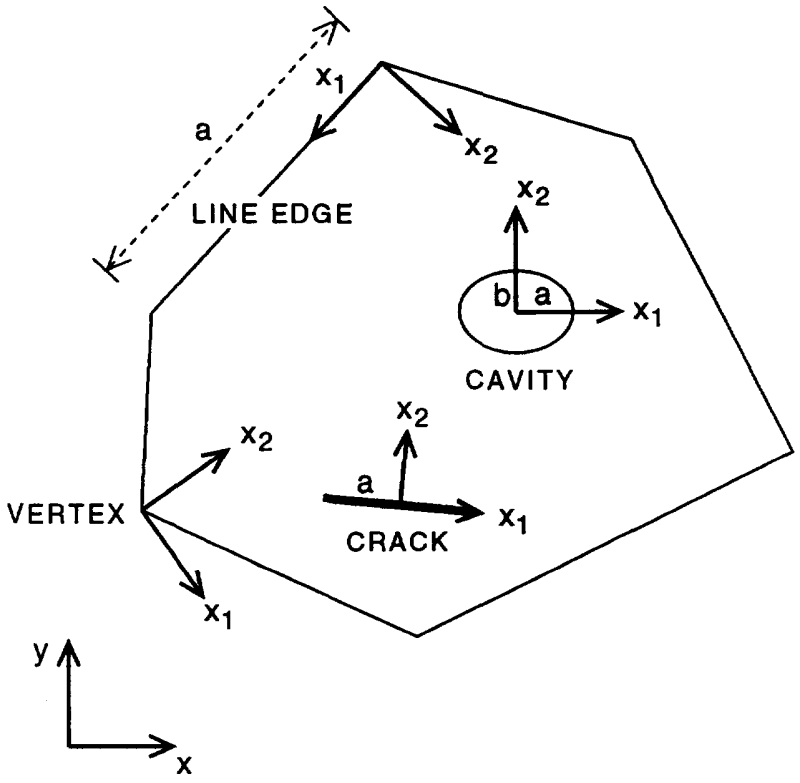

Fig. 1. Finite polygonal region (deforming in plane strain) containing an elliptical cavity and a crack.

$$\sum_{i=1}^{6} c_i \mu^i = 0. \tag{8}$$

The coefficients, s_{ijk}, p_{ik} and c_i in eqns (6), (7) and (8), respectively, are functions of the compliance components $a_{ij}(i,j = 1\text{–}6)$. If the body has a plane of symmetry normal to the generators (x_3-axis), it can be shown that the body deforms in a *plane strain* manner and that the displacement and stress components depend on $\Phi_1(z_1)$ and $\Phi_2(z_2)$ only.

The significance of the above formulation is that the solution of a boundary value problem in elasticity is reduced to the determination of appropriate analytical stress functions which satisfy the equilibrium eqns (5). The particular forms of these stress functions used in this study are briefly described in the next section.

3. POTENTIAL FUNCTION REPRESENTATION

Finite polygonal regions deforming in *plane strain*, such as the one shown in Fig. 1, are considered. The regions may contain circular or elliptical holes as well as cracks. In the edge function method, for a given polygonal region, the functions $\Phi_k(z_k)$ $(k = 1, 2)$ appearing in eqns (6) and (7) are expressed as follows

$$\Phi_k(z_k) = \sum_{n=1}^{N} \sum_{m=1}^{M_n} A_{kn}^m \Phi_{kn}^m(z_k) \tag{9}$$

where $\Phi_{kn}^m(z_k)$ are analytic functions which satisfy the homogeneous form of the equilibrium eqns (5) and A_{kn}^m are arbitrary constants which must be chosen to satisfy the boundary conditions of the region as well as possible. The rationale of the method is to choose functions $\Phi_{kn}^m(z_k)$ which are capable of representing the solution in the neighborhood of critical parts of the region boundary such as straight line segments, angular corners (vertices)

and interior cavities. In eqn (9), N is the number of such critical parts and M_n is the number of potential functions associated with critical part n. In general, the solution for each critical part is an infinite series truncated at M_n terms.

Particular forms of the potentials $\Phi_{kn}^{m}(z_k)$ associated with each critical part of the boundary of the region of interest are described in detail in Dwyer (1986) and Dwyer and Amadei (1995a,b). Certain potentials are used to model arbitrary displacements or tractions on each straight line edge or cavity edge of the region and are termed *edge functions*. System matrix stability considerations require that each edge function displacement and traction field decays away from the boundary with which it is associated. A limiting form of the cavity edge function is used as a crack edge function. The corresponding derivatives display the correct square root singularity behavior. Singular solutions which satisfy homogeneous boundary conditions in the neighborhood of a vertex are included in the representation of the approximate solution in order to accelerate convergence. Such solutions are termed *vertex functions*. Potentials which model arbitrary (aperiodic) effects on each edge and which yield displacements/tractions which are non-zero at the ends of each edge must also be included and these are known as *polar functions*.

A particular solution, corresponding to a gravity body force term, was developed in Dwyer and Amadei (1995a). This solution is subtracted from the original problem to give a modified boundary value problem which satisfies the homogeneous form of the equilibrium eqns (5).

4. MATCHING THE BOUNDARY CONDITIONS

The representation of the approximate solution of the boundary value problem has the form given by (6) and (7) where the complex potentials, $\Phi_k(z_k)$, therein consist of linear combinations of edge functions, vertex functions and polar functions. Thus, the equilibrium eqns (5) are satisfied *a-priori* if appropriate particular integrals are subtracted to yield a modified problem with zero body forces. The only remaining step is to determine the coefficients appearing in the edge, vertex and polar function potentials from the boundary conditions of the boundary value problem. In this paper this is accomplished with the boundary galerkin method, which is based on an abstract principle of virtual work, and is equivalent to the minimization of the strain energy error in the case of traction or displacement problems. This minimization leads to a system of equations which can be solved for the vector of coefficients of the potentials. The system matrix is symmetric and positive definite for displacement or traction problems. Full details can be found in Dwyer (1986).

Boundary values and errors of the approximate solution are computed at a number of equidistant points on each boundary. The errors are computed in terms of the differences (residuals) between the prescribed and computed quantities at each of these points. For convenience, the root mean square of the residuals is used as a concise measure of accuracy. Displacements and tractions on specified lines and curves may also be computed.

The relationship between the potential functions and the number of degrees of freedom in a given problem is described in Dwyer and Amadei (1995a). In general, each approximating function in eqn (9) has a complex constant (two real constants) associated with it, for $k = 1$ and $k = 2$, thus giving rise to four degrees of freedom for each function.

5. ASSUMPTIONS

A vertical slice from a glacier is modeled as a two dimensional boundary value problem. It is assumed that the out-of-plane strain is equal to zero. This plane strain assumption of no deformation along the out-of-plane direction is justified since the geometry is considered sufficiently uniform in the direction perpendicular to the plane. It also implies that the out-of-plane stress is constant.

In order to model realistic features, the slice of the glacier is generally taken as 5000 meters long and 1000 meters high and sloped at 5° to the horizontal as shown in Fig. 2. The stresses σ_{nn} and σ_{tt} in directions perpendicular and parallel, respectively, to the top surface are calculated. Crevasses are introduced in the form of notches. These notches are

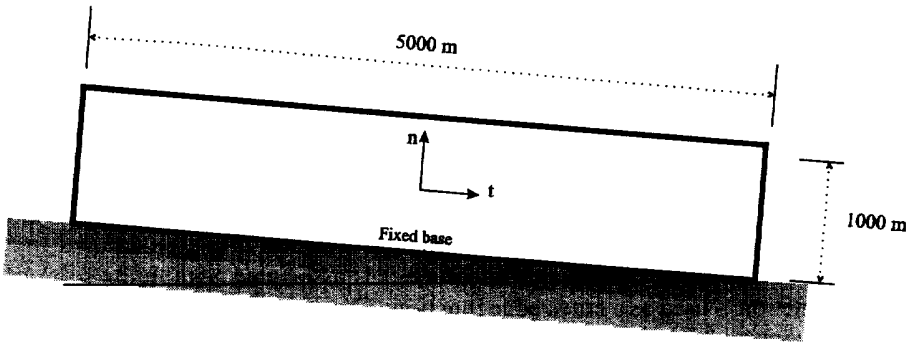

Fig. 2. Planar slice of a glacier, fixed at the base and free on all other sides.

relatively wide and are used to examine the re-distribution of stress following the initiation of crevasses. More realistic narrower notches have been considered in a concurrent BEM study (Sassolas *et al.*, in press).

In most of the examples presented herein the glacier is considered to be fixed as its base and free at the upstream, downstream and upper boundaries. The case of a fixed upstream boundary is examined but it is shown that the changed boundary condition does not have a significant effect on the stress pattern away from that end. A basal sliding condition may also be of interest and such a situation is being modeled in the BEM study.

Unless otherwise stated, Young's modulus for glacier ice is taken as $E = 11.8$ GPa and Poisson's ratio is taken as $\nu = 0.49$. This is a close approximation to the values for an incompressible ice. The exact value of $\nu = 0.5$ is not used because of the possibility of some numerical complications. The density of ice, denoted by ρ, is assumed to be 1000 kg/m^3 and the acceleration due to gravity, denoted by g, is taken to be 10 m/s^2.

Finally, the restriction to linear elastic behavior is in itself a major assumption. However, while ice deforms in non-linear creep at low stresses, elastic behavior dominates at high stress and in fracture. Further studies are expected in the near future in which one of the elastic modeling programs, the DDA model, will be modified to take account of viscoelastic constitutive behavior.

6. EXAMPLES

Example 1

This first case involves a 5000 m by 1000 m vertical slice from a glacier which is sloped at 5° to the horizontal. It is fixed at the base and free on the other three boundaries. The only active force is that due to gravity. The problem was modeled using three harmonic levels each of Polar functions and Edge functions and 17 vertex functions giving a total of 76 degrees of freedom. The most significant vertex functions in the representation are the vertex functions used to model the singularities at each of the corners of the base. The solution was obtained with a maximum root mean square residual of 1.1% of ρgH where $H = 1000$ m is the maximum height (thickness) of the glacier. This level of residual indicates that a highly accurate solution is obtained. Fig. 3(a) shows a contour plot of the stresses, σ_{nn}, normal to the top surface of the glacier. This is included mainly for verification purposes and it is clear that a uniform gravity pattern is obtained as expected. The stresses, σ_{tt}, normal to the sides of the slice are of greater interest and are displayed in Fig. 3(b). Roughly-one quarter of the glacier is seen to be in a state of tension while the lower three-quarters is in compression.

Example 2

The effect of choosing different lengths for the representative slice of the glacier is studied in this example. All of the parameters are the same as in Example 1 except that lengths of 2000 m and 10,000 m are chosen. The same number of degrees of freedom are used here as in Example 1. The maximum root mean Square residual for the 2000 m long

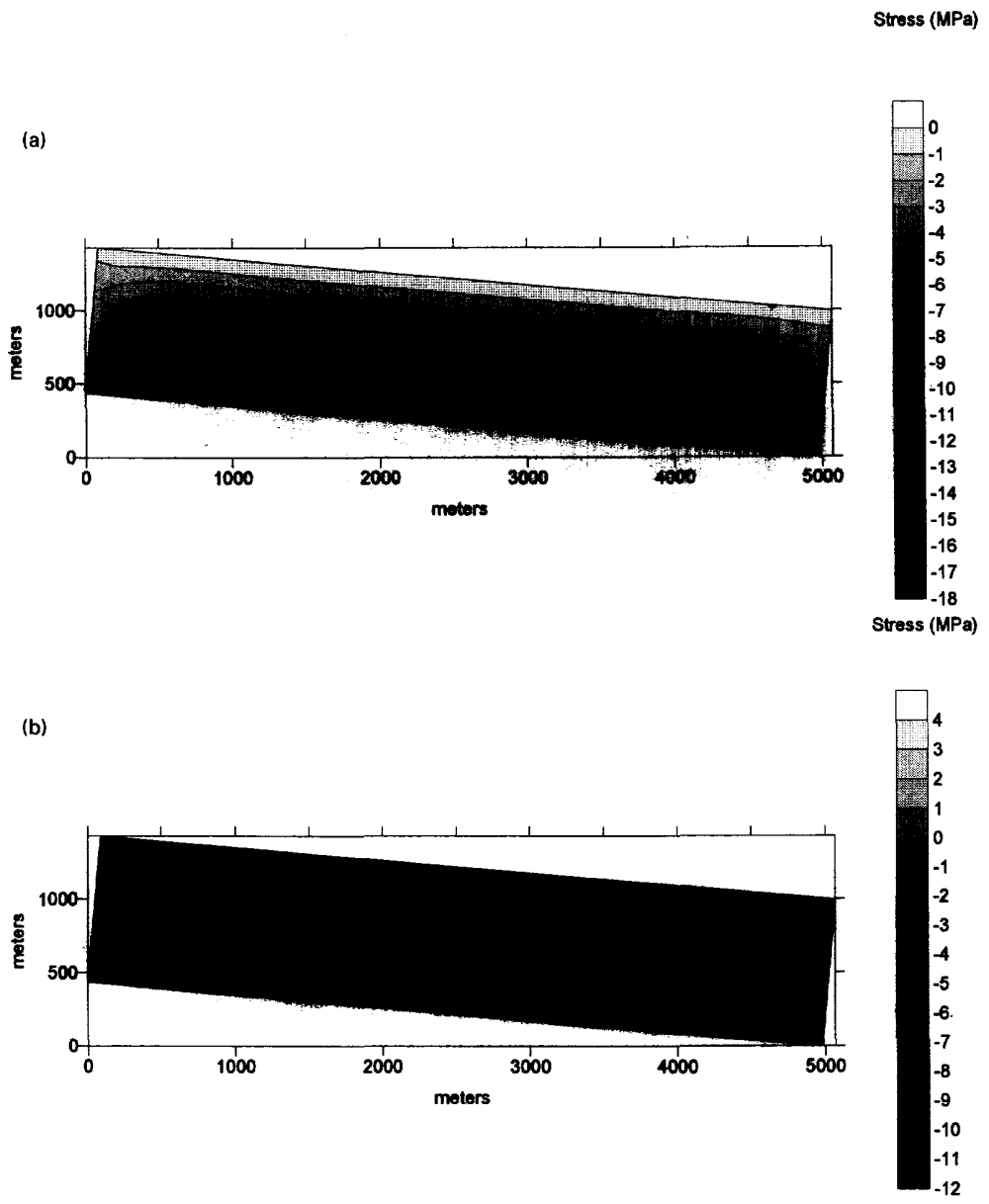

Fig. 3. (a) σ_{nn} stress contours in a 5000 m × 1000 m slice of a glacier. (b) σ_{tt} stress contours in a 5000 m × 1000 m slice of a glacier.

slice was 0.2% of ρgH and for the 10,000 m long case it was 2.6% of ρgH. The longer slice is slightly more difficult to model but nevertheless an accurate solution is obtained.

Figure 4(a) shows the σ_{tt} stress contours for the shorter slice. There is a larger area of tension clearly shown in the upper part of the slice. The corresponding display of σ_{tt} for the 10,000 m long glacier is shown in Fig. 4(b). The pattern is quite similar to that displayed in Fig. 3(b) for the 5000 m long slice. In particular, the area of maximum tension is the same—located approximately one glacier height way from the terminus.

In view of the results of this example, it was decided that a 5000 m long slice was sufficiently long to represent a realistic glacier. It is also clear that the 2000 m long slice gives a stress pattern which is different and therefore should not be used. Thus, all of the subsequent examples utilize the 5000 m by 1000 m slice.

Example 3

The geometry and material parameters considered here are identical to those of Example 1. However in this case the upstream end is fixed. Five harmonic levels of Polar functions

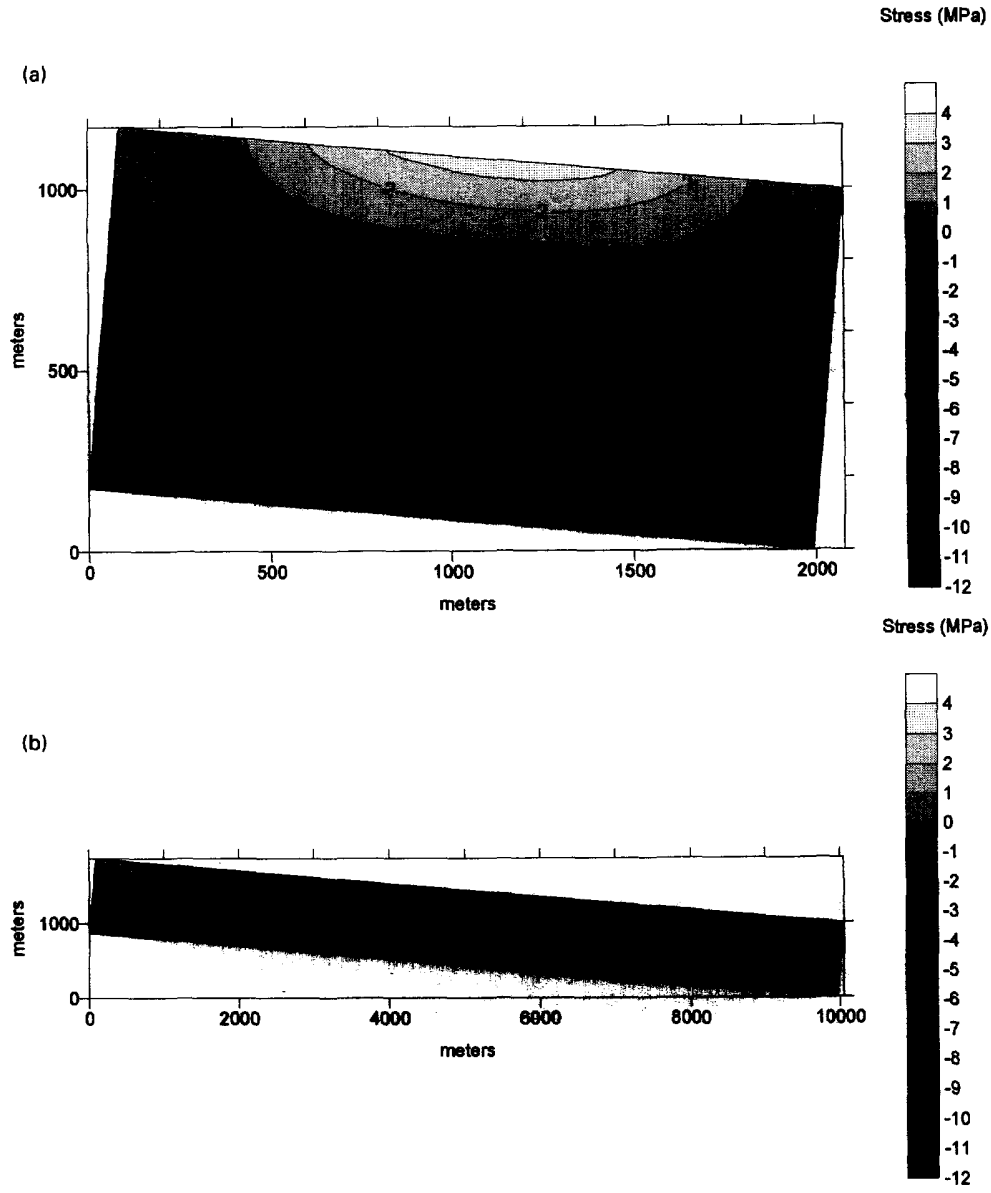

Fig. 4. (a) σ_{11} stress contours in a 2000 m × 1000 m slice of a glacier. (b) σ_{11} stress contours in a 10,000 m × 1000 m slice of a glacier.

and Edge functions were used in the approximation, together with 21 vertex functions, giving a total of 120 degrees of freedom. Maximum root mean square residuals in this example were 0.34% of ρgH.

Figure 5 shows the σ_{11} stress contours for this case. A comparison with Fig. 3(b) shows that the fixing of the upstream end only affects the stress pattern near that end, in particular a diminishing of the area of higher tension at the surface. Away from the fixed end the stresses are similar in both diagrams, although some reduction in tension can be observed along much of the surface. This suggests that in a long narrow glacier the end effects are not important in producing an overall stress pattern. The higher tension observed near the fixed boundary in Example 1 may simply be a product of the somewhat artificial free boundary condition. Nevertheless, since the overall pattern away from that end is unchanged, it was decided to proceed with the investigations using the parameters and boundary conditions from Example 1. However, one should be cautious in interpreting results along the surface within about 3.5 glacier thickness of the upstream end.

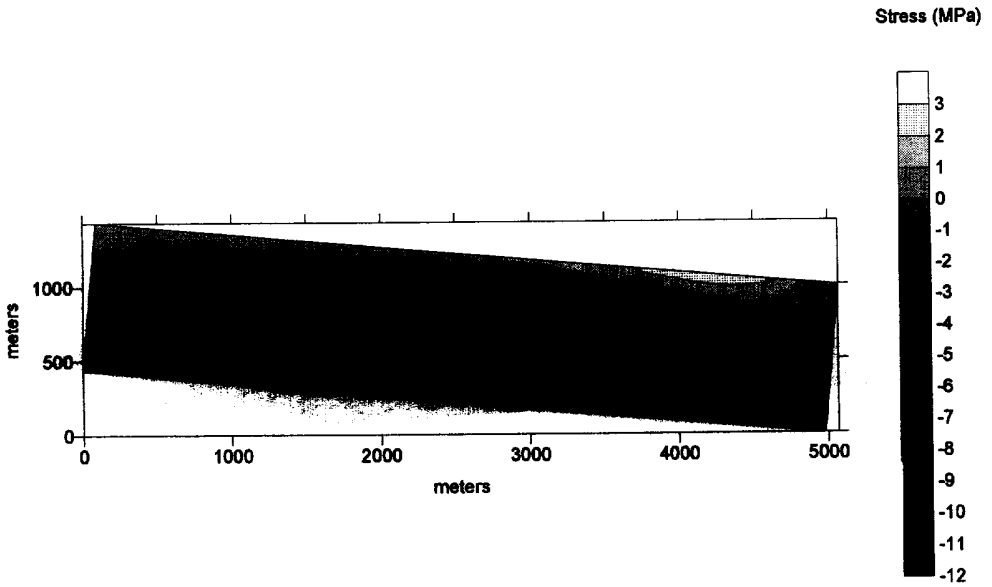

Fig. 5. σ_{tt} stress contours in a 5000 m × 1000 m slice of a glacier. Left end is fixed.

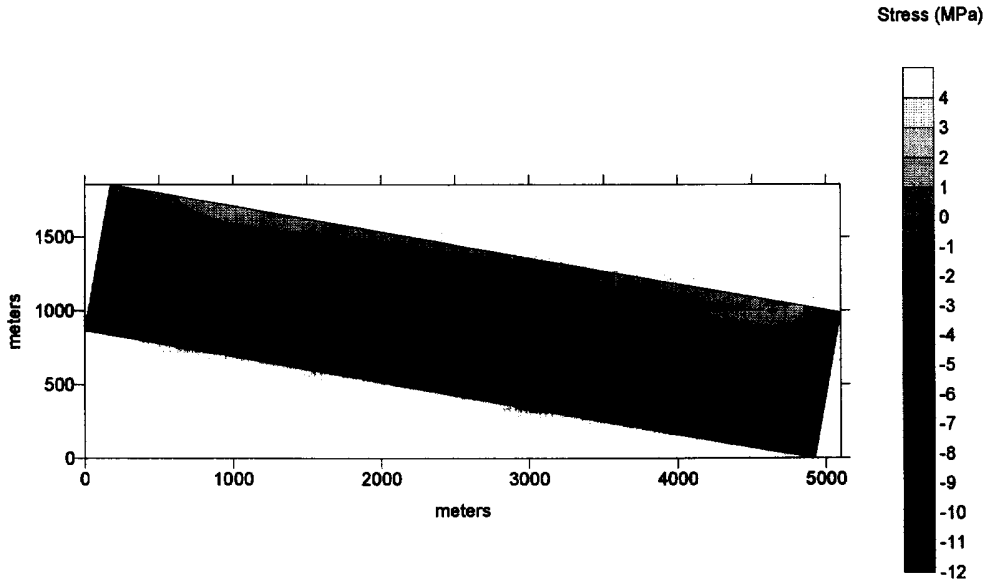

Fig. 6. σ_{tt} stress contours in a 5000 m × 1000 m slice of a glacier. Glacier is sloped at 10° to the horizontal.

Example 4

The only difference between this example and Example 1 is that the glacier is now sloped at 10° to the horizontal. An accurate solution, with maximum root mean square residuals of 0.26% of ρgH, was obtained using 116 degrees of freedom. The σ_{tt} stress pattern is shown in Fig. 6 and it is clear that there is no significant difference between this pattern and that displayed in Fig. 3(b) for the case of a 5° slope. The implication is that minor variations in the slope of a glacier do not have a major impact on the variation of the σ_{tt} stress and the corresponding tendencies to form crevasses.

Example 5

Although ice is generally treated as being close to incompressible, with a Poisson's ratio of $\nu = 0.5$, it is interesting to examine the variation of Poisson's ratio. Otherwise, in this example, the geometry and material are the same as in Example 1. Two situations are

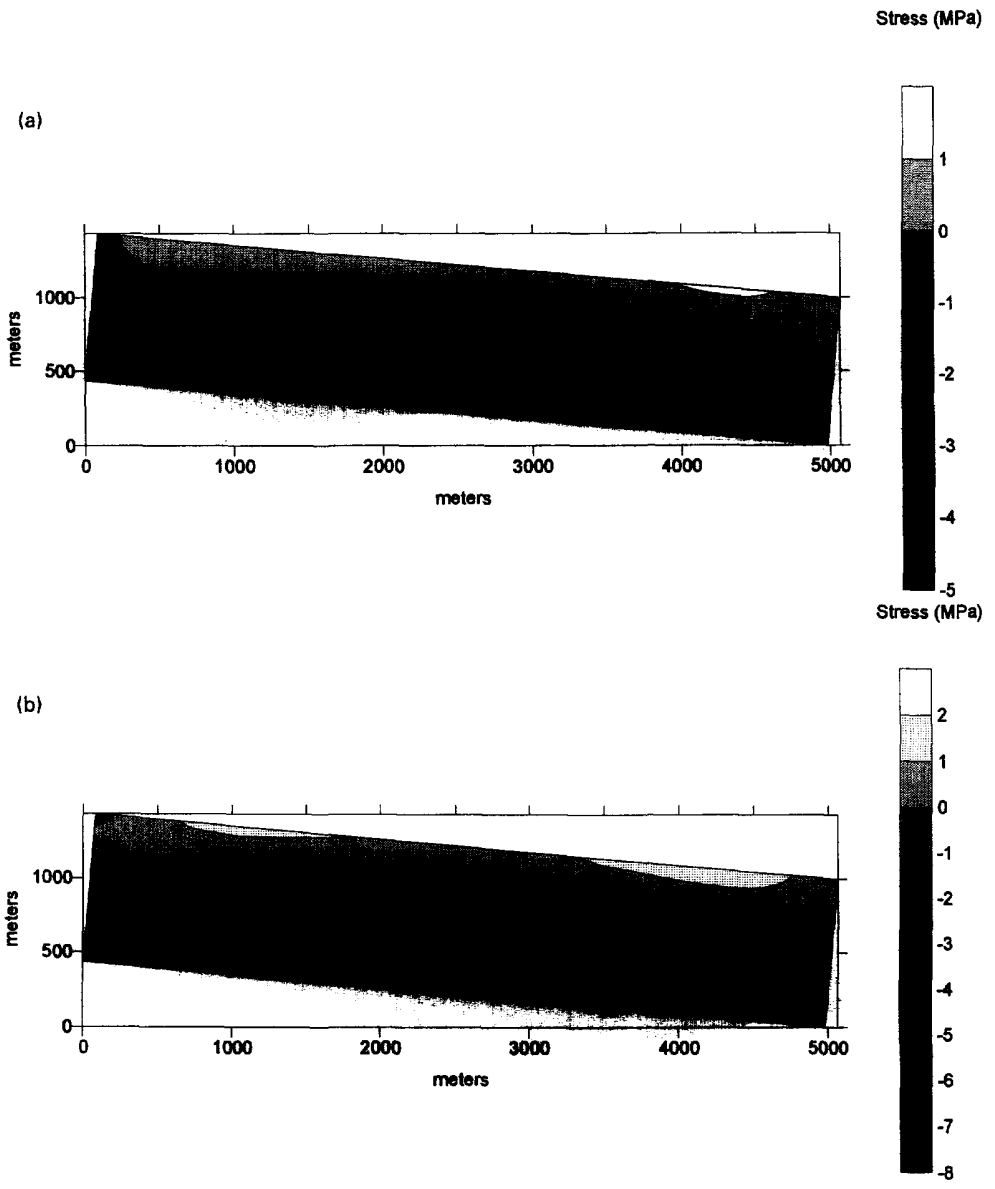

Fig. 7. (a) σ_{tt} stress contours in a 5000 m × 1000 m slice of a glacier. Poisson's ratio, $\nu = 0.3$. (b) σ_{tt} stress contours in a 5000 m × 1000 m slice of a glacier. Poisson's ratio, $\nu = 0.4$.

considered and in both cases 75 degrees of freedom were used. In each instance the maximum root mean square residuals were less than 1% of ρgH.

Contour plots of σ_{tt} for $\nu = 0.3$ and $\nu = 0.4$ are shown in Figs, 7(a) and (7b), respectively. The areas of tension are not appreciably different from those in Fig. 3(b) for $\nu = 0.49$. The major difference is in the magnitude of the σ_{tt} stresses, which become smaller as the Poisson's ratio is reduced. Indeed, for the case of $\nu = 0.3$ the maximum horizontal stresses are only about one half of those displayed for $\nu = 0.49$. In the latter case the magnitude of σ_{tt} is comparable to that of σ_{nn}. This suggests that there would be a greater tendency towards fracture initiation on the surface of a more incompressible material. As a result, caution must be exercised when choosing an appropriate value of Poisson's ratio in any numerical investigation.

Example 6

The 5000 m by 1000 m slice of a glacier is considered again. The material parameters and boundary conditions are identical to those in Example 1. However, at this stage a

notch, of width $W = 500$ m and depth $d = 250$ m, is introduced into one of the areas of higher tension in order to simulate the effects of a crevasse on the pattern of stress within the glacier. The position and dimensions of the notch are indicated in Fig. 8(a).

Three harmonic levels of Edge functions and Polar functions are used in the approximation, as well as 35 vertex functions. The most critical functions in this representation are those vertex functions used to model the singularity at the tip of the notch. The total number of degrees of freedom is 130 and this led to an accurate solution with a maximum root mean square residual of 2.8% of ρgH.

The effect of the notch on the distribution of the σ_{tt} stress is exhibited in Fig. 8(a). It is clear that the area of tension near the terminus is dissipated, but equally clear that the tension is not altogether removed. Furthermore, there is of course a concentration of stress at the tip of the notch. There is no reduction in the area of tension at a distance of $2W$ away from the notch. The implication of these plots is that the presence of a single small notch may not have sufficient effect to reduce tension and the associated tendency for further crevasse initiation.

The effect of a notch in another position on the surface of the glacier was also examined. The dimensions are indicated on Fig. 8(b), which also displays the σ_{tt} stress contours. As in the previous case, 130 degrees of freedom were used and a maximum root mean square residual of 1.4% ρgH was observed for the solution obtained. This clearly indicates that an accurate approximation is achieved. The stress plot shows that the extent of the effect of this notch is limited in a manner similar to the other notch.

Another effect to be considered is the obviously high stress concentration apparent at the tip of the notch in Fig. 8(a)—while the tip remains in an area of tension the crevasse should continue to propagate. Indeed this stress concentration at the tip is as great as any stress on the surface, suggesting the possibility of continued propagation of an existing crevasse rather than the initiation of new crevasses—an expected result in any applied mechanics context.

Given the possible question regarding the suitability of the edge function approach for such a notch problem, it is informative to compare the solution with that obtained from the finite element method (SAP, 1990). A combination of eighty (80) constant strain elements throughout the slice and thirty (30) quadratic strain elements near the tip of the crevasse were used in the finite element model. This resulted in 163 nodes or 326 degrees of freedom. The σ_{tt} stress contours from this model are displayed in Fig. 8(c). A comparison with the corresponding edge function results in Fig. 8(a) indicates that the tension at the tip of the crevasse is captured more accurately by the edge function method. Furthermore there is no convenient measure of the error in the finite element analysis. It is finally worth mentioning that the setup of the finite element mesh in this instance took several hours to accomplish, in contrast to a much shorter time required for the corresponding edge function model.

Example 7

This example considers the case of two crevasses, introduced as two notches at the positions indicated in Figs 9(a) and 9(b). Three levels of Polar functions and Edge functions are utilized together with 53 vertex functions, giving a total of 184 degrees of freedom in this instance. Once again a very accurate solution is obtained with a maximum root mean square residual of 0.88% of ρgH.

Contour plots of σ_{nn} and σ_{tt} are shown in Figs 9(a) and 9(b) respectively. A comparison with Figs 3(a) and 3(b) clearly shows that the effects of the notches are similar to those mentioned above for the single individual notches. The conclusion must be that the introduction of a small number of widely spaced crevasses does not inhibit the initiation of further crevasses formed due to areas of high tension on the surface of a glacier. Of course, the tendency of existing crevasses to propagate is also high, as mentioned in the previous example.

Example 8

As the ratio of notch width to depth is decreased it has been observed that the edge function method results in higher residuals. This is due to the fact that line edge functions

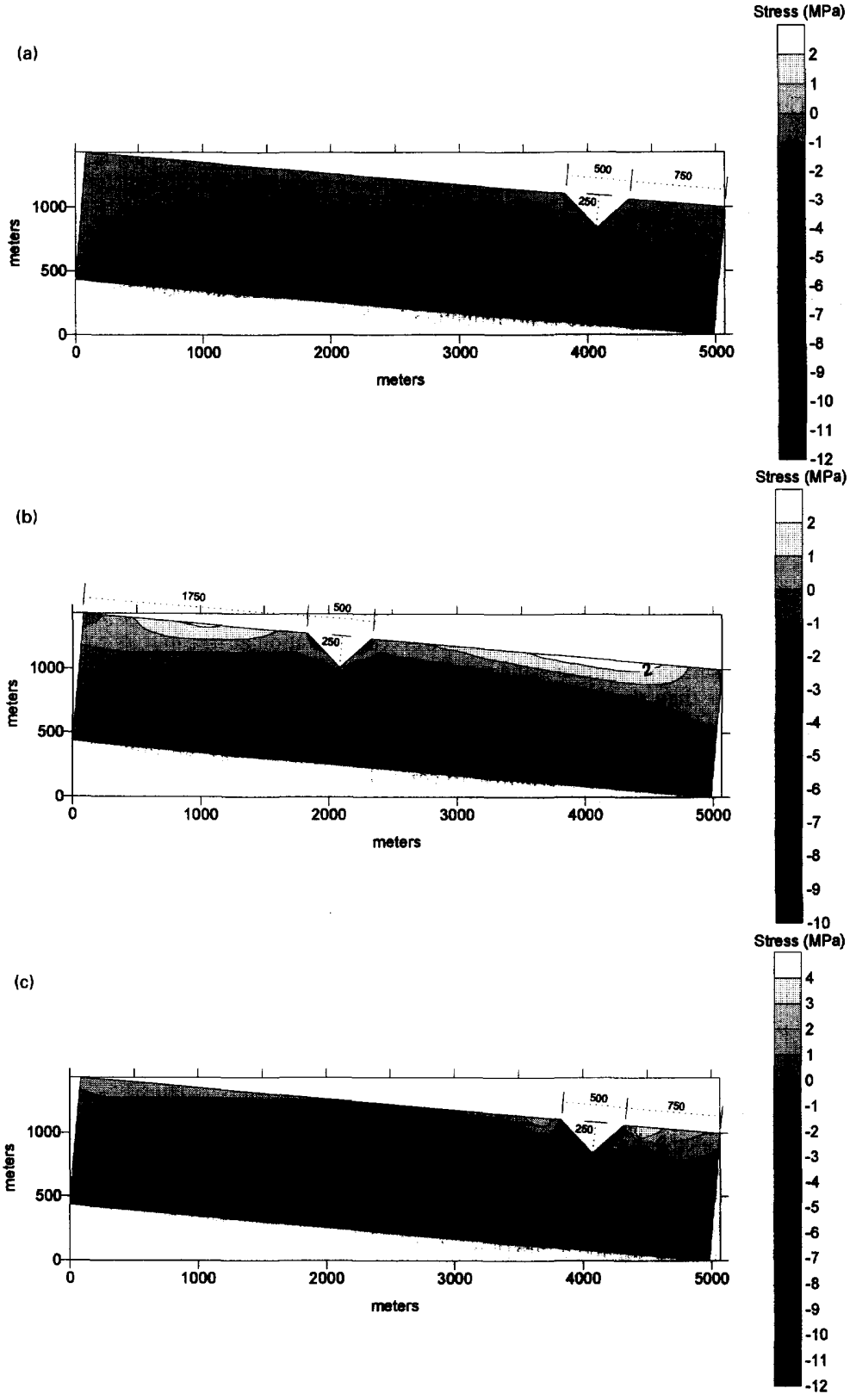

Fig. 8. (a) σ_{tt} stress contours in a 5000 m × 1000 m slice of a glacier with a crevasse near the terminus. (b) σ_{tt} stress contours in a 5000 m × 1000 m slice of a glacier with a crevasse near the centre. (c) σ_{tt} stress contours in an 5000 m × 1000 m slice of a glacier with a crevasse near the terminus. Contours obtained from finite element analysis.

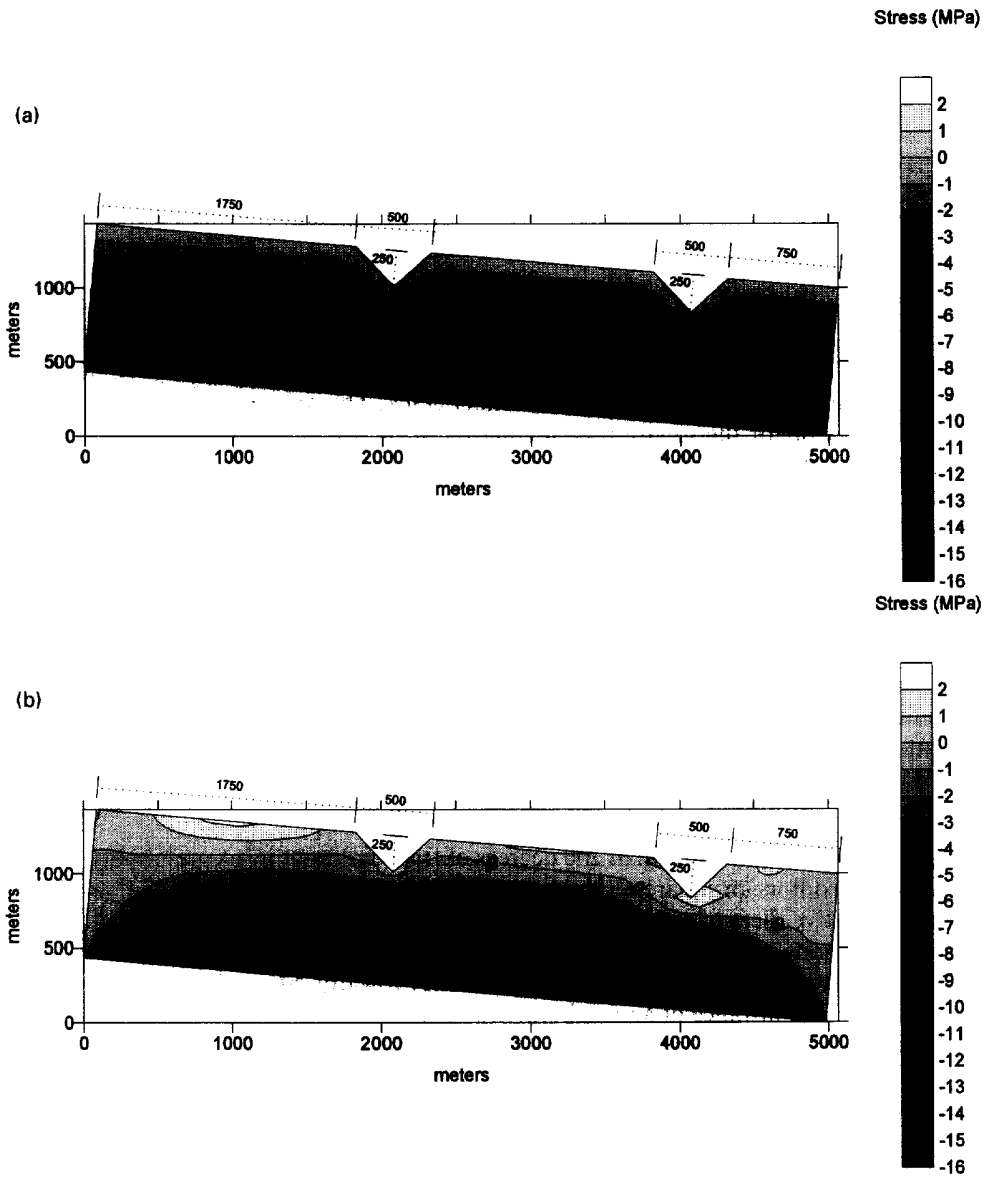

Fig. 9. (a) σ_{mm} stress contours in a 5000 m × 1000 m slice of a glacier with two crevasses. (b) σ_{tt} stress contours in a 5000 m × 1000 m slice of a glacier with two crevasses.

on one side of a notch have a significant effect on the opposite side of the notch as the decay factor for such functions only operates inwards to the region modeled. This limits the use of the method for regions with re-entrant angles. In order to examine such behavior, and to assess the limitations of the program for crevasse modeling, a convergence study was undertaken, in which a simple notch in a flat slab of ice was examined. Approximately 195 degrees of freedom were used in this study. This notch was centrally placed on top of a 5000 m by 1000 m slice and the ratio of notch width (W) to notch depth (d) was varied. The resulting errors in the form of the maximum observed values of the root mean square residuals are shown in Table 1. It is clear that the results become unacceptable when the W/d ratio is lower than 2. For this particular geometry even the 2.5 ratio gave a poor result. However, each of the cases used above in the parametric studies had acceptable residuals, as quoted in those examples.

The program also computes parameters related to the vertex functions which model the singularity at the tip of the crevasse. One of these parameters measures the nature of that singularity and it is interesting to note from Table 1 that the singularity at the tip is

Table 1. Errors in analysis of notch problem

W/d	Vertex singularity parameter	% root mean square residual
4.0	0.639	0.63
3.5	0.618	0.53
3.0	0.593	4.10
2.5	0.569	11.00
2.0	0.544	2.10
1.5	0.523	21.60

well captured by the vertex functions as it is clear that the appropriate term is approaching 0.5 as the notch approaches the form of a slender crack. This value of course represents the required behavior for the square root singularity at the tip of a crack. This suggests that the modeling difficulty is indeed due to the line edge function effect mentioned above, and not due to any difficulty with the singularity.

7. DISCUSSION AND CONCLUSIONS

The major purpose of the investigations reported in this paper was to obtain stress patterns for a range of aspect ratios and crack geometries. The edge function method is appropriate for achieving highly accurate solutions for certain problems and this study was limited to such cases. Therefore it must be emphasized that all of the results presented are accurate and that the trends displayed are a reliable representation of the stresses for the limited cases examined.

The main conclusions are:

1. Approximations using less than 200 degrees of freedom result in accurate solutions with maximum root mean square residuals less than 3% of ρgH.
2. Representative slices of a glacier need to be of the order of 5000 m by 1000 m to provide a realistic model; aspect ratio is important.
3. The greatest tension and the consequent tendency towards crevasse initiation occurs on the surface at a distance of approximately one glacier height away from the terminus.
4. Variations in the slope of the glacier from 5° to 10° do not greatly affect the stress pattern.
5. Higher values of the σ_{tt} stresses are obtained as the value of the Poisson's ratio is increased to approach $\nu = 0.5$, corresponding to an incompressible material.
6. The presence of one or two widely spaced notches does not seem to significantly reduce the tension on the surface of a glacier away from those notches.
7. The tendency of existing crevasses to propagate is as high as any tendency towards initiation of new crevasses.
8. The method is currently limited to situations where the ratio of crevasse width to depth is greater than 2.

The conclusions listed may be stated with confidence because of the accuracy of the results obtained. However that accuracy deteriorates as the crevasses are placed closer together or increased in number. Furthermore the modeling of more physically realistic narrower crevasses is also problematic. An investigation, using the BEM method, to examine the effects of crevasses upon one another and their dependence upon spacing ratios, is currently underway and such an approach seems more promising for tackling these issues.

Since the edge function method is limited to certain geometries and lacks robustness as a general model its optimum use may be as a special element within a conventional finite element code. The high accuracy achieved in the edge function work can complement the finite element method's generality of geometry and boundary conditions. A particular coupling of this nature is being studied at present in order to use the edge function method to model local fracture behavior, while using a finite element program to model the overall movement and deformation of the glacier.

Acknowledgements—This work was supported by the Department of Energy under grant DE-FG 03-93-ER61689.

REFERENCES

Dwyer, J. F. (1986) Application of the edge function method to singular plane problems in anisotropic elasticity. Ph.D. Thesis, University College Cork.

Dwyer, J. F. and Amadei, B. (1995a) Application of the edge function method to rock mechanics problems. *Rock Mech. and Rock Engng* **28**(4), 185–209.

Dwyer, J. F. and Amadei, B. (1995b) The edge function method and singular problems in rock mechanics. *Int. J. Rock Mech. Min. Sci. Geom. Abs.* **32**, 121–133.

Fastook, J. L. and Chapman, J. E. (1987) A map-plane finite element model: three modeling experiments. *J. Glaciol.* **35**, 48–52.

Grannell, J. J. and Dwyer, J. F. (1989) Numerical solution of anisotropic linear elastic fracture problems. *Key Engng Mat.* **32**, 115–120.

Grannell, J. J. and Quinlan, P. M. (1980) The edge function method for thin anisotropic plate bending. *Proc. Roy. Irish Acad.* **80A**, 1–22.

Grannel, J. J., Quinlan, P. M., Atluri, S. N. and Fitzgerald, J. E. (1979) Boundary discretization using the edge function method in three dimensional elasticity. *Appl. Math. Mod.* **3**, 18–24.

Hocking, G., Williams, J. R. and Mustoe, G. G. W. (1985) Dynamic global forces on an offshore structure from multi-year ice floe impacts. In *ASCE Speciality Conf.*, San Fransicsco, CA, 25–27 March 1985 (eds Bennet, F. L. and J. L. Machemehl), ASCE, New York, pp. 202–210.

Holdsworth, G. (1969) Flexure of a floating ice tongue. *J. Glaciol.* **8**, 385–397.

Holdsworth, G. (1977) Tidal interaction with ice shelves. *Ann. Geophys.* **33**, 133–146.

Hooke, R. L., Mellor, M. *et al.* (1980) Mechanical properties of polycrystalline ice; an assessment of current knowledge and priorities for research. *Cold Regs Sci. Tech.* **3**, 263–275.

Hughes, T. (1983) On the disintegration of ice shelves: the role of fracture *J. Glaciol.* **29**, 98–117.

Hughes, T. (1992) Theoretical calving rates from glaciers along ice walls grounded in water of variable depths. *J. Glaciol.* **38**, 282–294.

Lekhnitskii, S. G. (1963) *Theory of Elasticity of an Anisotropic Elastic Body*. Holden-Day.

O'Callaghan, M. J. A. and Studdert, R. P. (1985) The edge function method for free vibrations of thin orthotropic plates. In *Boundary Elements VII. Proc. Int. Conf.* (eds Brebbia, C. A. and G. Maier), Springer, Berlin, pp. 6.37–6.52.

Quinlan, P. M. (1964) The torsion of an irregular polygon. *Proc. Roy. Soc.* Vol. A282, pp. 208–227.

Raymond, C. F. (1978) Numerical calculation of glacier flow by finite element methods. *Final Tech. Rep. for NSF Grant DPP*74-19075, unpublished.

Raymond, C. F., Johannesson, T., Pfeffer, T. and Sharp, M. (1987) Propagation of a glacier surge into stagnant ice. *J. Geophys. Res.* **92**, 9037–9049.

Reeh, N. (1968) On the calving of ice from floating glaciers and ice shelves. *J. Glaciol.* **7**, 215–232.

SAP 90 (1990) Computers and Structures, Inc., Berkeley, CA.

Sassolas, C., Pfeffer, T. and Amadei, B. (in press). Stress interaction between multiple crevasses in glacier ice. *Cold Regs Sci. Tech.*

Schulson, E. M., Hoxie, S. G. and Nixon, W. A. (1989) The tensile strength of cracked ice. *Phil. Mag.* **59**, 303–311.

Schulson, E. M. (1991) The tensile and compressive fracture of ice in ice-structure interaction. In *IUTAM-IAHR Symposium* (eds Jones, S., R. F. McKenna, J. Tillotson and I. Jordan), St. John's Newfoundland, Canada, Springer, Berlin-Heidelberg, pp. 165–187.